Liquid Crystals
Publication details, including instructions for authors and subscription information:
http://www.informaworld.com/smpp/title~content=t713926090

Ferroelectric side group liquid crystalline polysiloxanes containing a chiral sulphinate derivative

S. Mery; L. Catala; P. Sebastiao; B. Heinrich; J. F. Nicoud; D. Guillon

To cite this Article Mery, S. , Catala, L. , Sebastiao, P. , Heinrich, B. , Nicoud, J. F. and Guillon, D.(1999) 'Ferroelectric side group liquid crystalline polysiloxanes containing a chiral sulphinate derivative', Liquid Crystals, 26: 10, 1445 — 1454
To link to this Article: DOI: 10.1080/026782999203779
URL: http://dx.doi.org/10.1080/026782999203779

LIQUID CRYSTALS, 1999, VOL. 26, NO. 10, 1445–1454

Ferroelectric side group liquid crystalline polysiloxanes containing a chiral sulphinate derivative

S. MÉRY*, L. CATALA, P. SEBASTIÃO†, B. HEINRICH, J. F. NICOUD
and D. GUILLON

Institut de Physique et Chimie des Matériaux de Strasbourg,
Groupe des Matériaux Organiques, 23 rue du Loess, 67037 Strasbourg Cedex,
France
†Centro de Física da Matéria Condensada,
Universidad di Lisboa Av. Prof. Gama Pinto 2, 1649-003 Lisboa, Portugal
‡Instituto Superior Técnico, Av. Rovisco Pais, 1096 Lisboa, Portugal

(*Received 18 January 1999; accepted 7 April 1999*)

A series of chiral liquid crystalline homo- and co-polysiloxanes is reported, in which the chirality is introduced via an arenesulphinate moiety. All polysiloxanes were prepared by using three polymer-analogous reactions and exhibit the ferroelectric SmC* phase. In the series of copolymers, a high heterogeneity in the ratio of mesogenic pendants is observed and explains the existence of large biphasic regions at the phase transitions. A complete characterization of the ferroelectric properties was performed for the copolysiloxanes, and revealed high values of the spontaneous polarization.

1. Introduction

The search for new chiral moieties in ferroelectric liquid crystals is of considerable interest. The choice of a judicious chiral moiety together with its neighbouring groups can drastically enhance the transverse dipole moment of the mesogen and hence the macroscopic polarization of the mesophase [1]. Spontaneous polarization ($\mathbf{P}_s$) in liquid crystals is also strongly correlated with the optical purity of the mesogens, since $\mathbf{P}_s$ is found to increase (linearly or not) with the increasing enantiomeric excess (ee) of the molecules [2–4]. It is therefore essential to specify the optical purity or ee of liquid crystal materials when $\mathbf{P}_s$ values are reported [5]. So far, most of the work carried out in synthesizing new chiral groups is done on moieties in which (more or less) polarizable groups are connected to one or several asymmetric carbon centres [6, 7]. However, very little work has been done on novel sources of chirality, such as axial [8–14] or planar chirality [15, 16], or on chiral moieties in which the chirality is introduced via an asymmetric hetero-atom [17–23]. Even though novel chiral systems reported so far do not always lead to ferroelectric liquid crystals, they open up an exciting new field of interest in chiral liquid crystals, in general.

The knowledge gained on the versatility of chiral groups in ferroelectric liquid crystals has not yet been fully pursued towards ferroelectric liquid crystalline polymers. Besides the use of 'conventional' chiral moieties composed of one or several asymmetric carbon centres, there have been a few reports of chiral side group liquid crystalline (SGLC) polymers containing novel sources of chirality. For instance, by using a chiral cyclohexylidene moiety, Zentel *et al.* have synthesized a ferroelectric SGLC copolysiloxane exhibiting an axial chirality [14]. Chiellini *et al.* have reported a series of SGLC polyacrylates bearing chiral sulphoxide groups for which the sulphur atom is the asymmetric centre [24]. Later, in our group a series of homopolysiloxanes with chiral sulphinate-based pendants has been synthesized and shown to exhibit ferroelectricity [25]. Descheneaux *et al.* also reported series of polyacrylates containing ferrocenyl groups, these latter being obtained optically active, eventually [26].

Recently our group reported a number of low molar mass ferroelectric liquid crystal materials in which the chirality was obtained by introducing a chiral alkyl benzenesulphinate, sulphoxide or sulphinamide moiety [21–23]. Examples of these mesogens are presented in figure 1.

The choice of such chiral moieties was motivated by several peculiarities [20]: (i) the presence of a rigid steric coupling between the asymmetric sulphur atom and a strong dipole moment (the S=O bond bears a dipole moment of 5.8 Debyes); (ii) the direct connection of the asymmetric centre to the rigid aromatic core. As

---

*Author for correspondence; e-mail: mery@michelangelo.u-strasbg.fr

Journal of Liquid Crystals ISSN 0267-8292 print/ISSN 1366-5855 online ©1999 Taylor & Francis Ltd
http://www.tandf.co.uk/JNLS/lct.htm
http://www.taylorandfrancis.com/JNLS/lct.htm

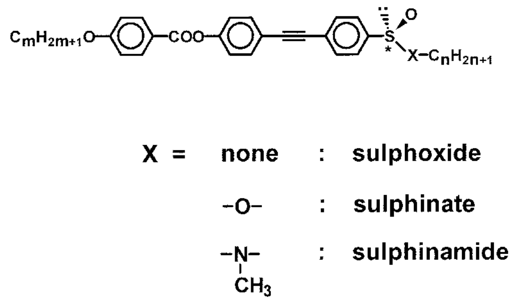

Figure 1. Chemical structure of ferroelectric liquid crystalline sulphinyl-based materials.

a result, high spontaneous polarization values (up to 270 nC cm^{-2}) could be measured for the SmC* phases of some of the mesogens of very high optical purity (ee ~ 100%) presented above [4].

The sulphinate-based mesogens exhibit the highest thermal stability and were used to prepare a series of SGLC homopolysiloxanes [25]. These polymers clearly revealed ferroelectricity but, because of their high viscosity and high transition temperatures, which made them sensitive to thermal degradation, no full characterization of the ferroelectricity was performed. In order to investigate the ferroelectric properties of such chiral sulphinate-based polymers, another series of materials having reduced viscosity and transition temperatures has been synthesized. These materials are SGLC copolysiloxanes, for which an average of 35% of the siloxane repeat units of the polymer backbone bear a mesogenic pendant. The molecular structure of the copolysiloxanes, as well as the homopolysiloxanes are depicted in figure 2. The acronyms used for naming the polymers are (*R*)-COPS 11-*n* for the copolysiloxanes and (*R*)-PS 11-*n* for the homopolysiloxanes, where 11 and *n* (with $n = 8$, 10 or 12) stand for the number of methylene segments in the spacer and the carbon number of the terminal alkyl chain, respectively. *R* stands for the configuration at the sulphur atom. The average ratio of the mesogenic pendants per siloxane repeat unit of the polymer is given by $x = a/(a + b)$, where a is the methylsiloxane repeat unit substituted by a mesogenic pendant and b is the dimethylsiloxane comonomer repeat unit.

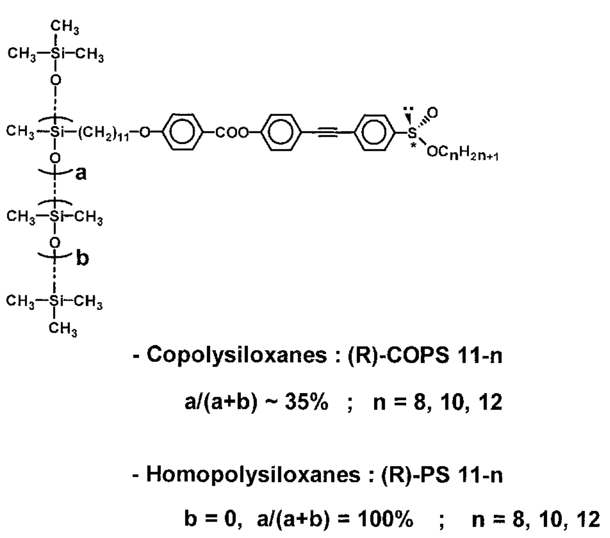

Figure 2. Chemical structure of sulphinate-based liquid crystalline co- and homo-polysiloxanes.

In this paper we report a brief description of the synthetic procedure used for the preparation of the SGLC copolysiloxanes having an arenesulphinate group as the chiral moiety. Evidence of a wide biphasic region at the clearing temperature is also presented. The emphasis of the present paper is given to the characterization of the mesomorphic and ferroelectric properties. Finally, a comparison of the mesomorphic properties of the SGLC copolysiloxanes with those of their analogous homopolysiloxanes is reported.

2. Synthesis

The synthetic route used for the preparation of the SGLC copolysiloxanes is outlined in scheme 1. The liquid crystalline polysiloxanes were prepared by using three successive polymer-analogous reactions, starting from commercially available poly(dimethylsiloxane-co-methylhydrogenosiloxane) chains. This procedure was chosen instead of the 'classical' direct hydrosilylation of the complete vinyl-ended mesogen with the silane functionalities of the polysiloxanes for the two following reasons: the presence of the ethynyl group was found to compete with the vinyl group in the hydrosilylation process, and the platinum catalyst efficiency was strongly affected by the presence of the sulphinate moiety. The first polymer-analogous reaction consists of a hydrosilylation to prepare a copolysiloxane bearing undecyloxybenzoic acid pendants protected by a methoxybenzyl group (COPS 11-COOB*n*). The protecting group was cleaved in the second step by catalytic hydrogenolysis. The 'acidic' polysiloxane thus obtained was polyesterified with the optically active alkyl 4-(4-hydroxyphenyl)-ethynylbenzenesulphinate derivatives in the last step. The sulphinate derivatives, for which the synthesis is outlined in scheme 2, were synthesized with predominantely the *R* configuration at the sulfur atom. The determination of the enantiomeric excess (ee) of these materials by ^1H NMR using a chiral shift reagent gave values of 85, 90 and 92%, for the molecules with octyl, decyl and dodecyl terminal aliphatic chains, respectively [21]. As has been checked in a previous study [25], the esterification conditions used for the preparation of the polymers does not affect the enantiomeric excess of the sulphinate moieties. Therefore, the final polymers are assumed to have the same ee as their optically active

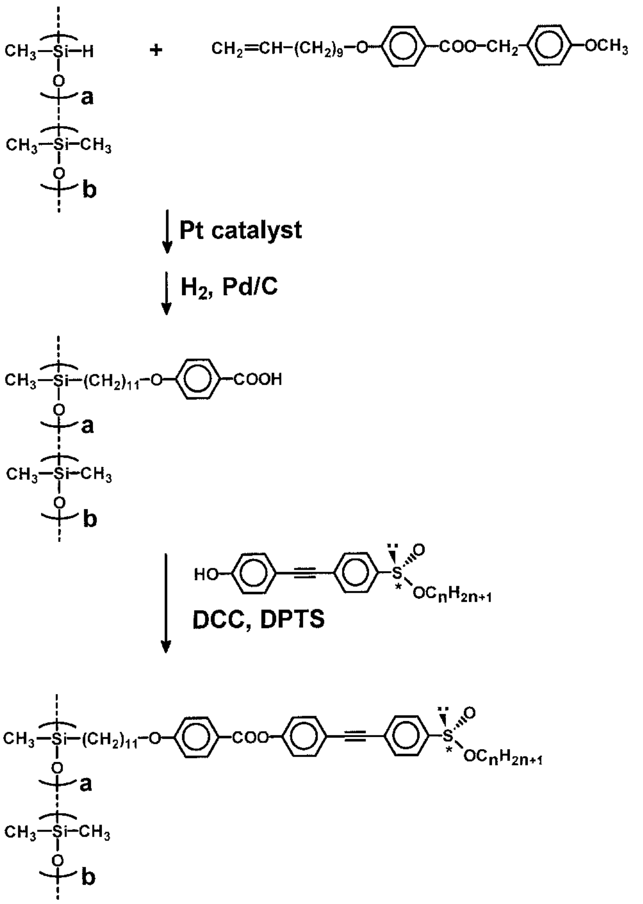

Scheme 1. Preparation of the sulphinate-based SGLC copolysiloxanes (*R*)-COPS 11-*n*.

precursors. The procedure involving three polymer-analogous reactions cited in the present paper has already been used for the preparation of the sulphinate-based liquid crystalline homopolysiloxanes (*R*)-PS 11-*n* [25]. For these more sterically packed systems, it was possible to obtain up to a 97% overall substitution of the siloxane units by the mesogenic moieties. The synthetic procedures for the polymer-analogous reactions are reported in §5. A more detailed description of these syntheses can be found elsewhere [25, 27].

3. Results and discussion

3.1. *Evidence for the wide distribution of the ratio of the mesogen pendants*

Preliminary mesomorphic investigations of one SGLC copolysiloxane, (*R*)-COPS 11-8, prepared as above revealed the presence of quite a large biphasic region (about 45°C) at the clearing point. The wide temperature range at the mesophase–isotropic transition was first suspected to be due to the presence of a wide polymer mass distribution. This is the reason why a systematic characterization of the polymers was performed, from the starting commercial copolysiloxane to the final SGLC polymer (*R*)-COPS 11-8. In table 1 the characteristics are reported of the polymers determined as explained in §5.

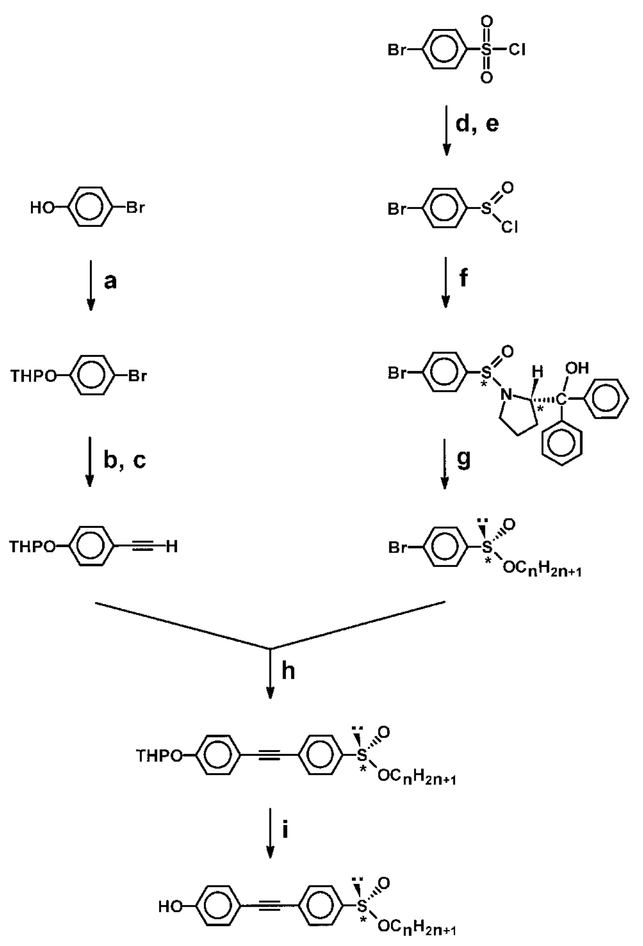

Scheme 2. Synthetic route for the preparation of the 4-*n*-alkoxysulphinyl-4′-hydroxytolane derivatives: (a) dihydro-4*H*-pyran, PTSA, CH_2Cl_2; (b) trimethylsilylacetylene, $PdCl_2$, $Cu(OAc)_2.H_2O$, triphenylphosphine, Et_3N; (c) TBAF, THF; (d) *p*-thiocresol, Et_3N/CH_2Cl_2; (e) $SOCl_2$; (f) (*S*)-(−)-α,α-diphenyl-2-pyrrolidinomethanol, toluene/pyridine; (g) $C_nH_{2n}OH$, TFA, toluene; (h) $PdCl_2$, $Cu(OAc)_2.H_2O$; triphenylphosphine, Et_3N; (i) pyridinium *p*-toluenesulphonate, MeOH.

The characteristics found for the starting copolysiloxanes ($M_n = 2050$, $x = 0.34$) are in agreement with those given by the manufacturer ($M_n = 2000$–2100, $x = 0.30$–0.35). Our analyses also revealed a relatively low value of the polydispersity ($I_p = 1.5$). For the substituted polymers, the variation of M_n was in accordance with the successive polymer-analogous reactions performed. The ratio of functionalized siloxane units (x) in the copolymers was found to increase after the hydrosilylation reaction and then to stabilize at a value of

Table 1. Characteristics of the copolymers. Materials are unfractionated when not mentioned. M_n = number-average molar mass, I_p = polydispersity index, x = average ratio of the functionalized siloxane units.

Materials	M_n	I_p	$x = a/(a + b)$
Commercial copolysiloxane	2050	1.5	0.34
COPS 11-COOB*n*	11 670	1.4	0.39
COPS 11-COOH	6260	1.5	0.37
COPS 11-COOH (fract.)	8870	1.35	0.38
(*R*)-COPS 11-8	19 880	1.9	0.38
(*R*)-COPS 11-8 (fract.)	18 300	1.4	0.38

about 0.38. Surprisingly, the value of I_p was found to increase in the last reaction step to reach a large value of 1.9 in the (*R*)-COPS 11-8.

In order to obtain better defined SGLC copolymers, we decided to reduce the polydispersity of the polymers further by performing a fractionation of the intermediate copolyacid COPS 11-COOH, from which the series of SGLC copolysiloxanes is prepared. As can be seen from table 1, the fractionation process reduced I_p from 1.5 to 1.35 in the copolyacid, which further led to a lower I_p value ($I_p = 1.4$) for the final SGLC copolysiloxanes—as compared with 1.9 in the unfractionated (*R*)-COPS 11-8. During the fractionation, x was found to be unchanged ($x = 0.38$). The chromatogram corresponding to the fractionated copolyacid is given in figure 3.

Surprisingly however, in spite of the low I_p value obtained for the fractionated SGLC copolysiloxanes, investigation of the thermal properties of the materials still revealed a large biphasic region (over 30°C) at the clearing temperature. Undoubtedly, the large biphasic gap at the transition could not now be due to a large polydispersity. Instead, the presence of a wide heterogeneity in the ratio of mesogenic pendants was strongly suspected. Indeed, it has to be pointed out that our polymers should really be considered as oligomers ($DP \sim 30$) and are only partially substituted ($x = 0.38$). As a result, each polymer chain bears an average of nine mesogenic pendants. It is, therefore, obvious that the mesomorphic properties of the copolymers would be strongly affected by both a large I_p and a heterogeneity in the degree of functionalization (x). One can reasonably estimate too that a heterogeneity in x would have a bigger effect on the thermal properties than a large I_p. The presence of heterogeneity in the degree of functionalization in our copolymers could finally be observed. During the fractionation process of the copolyacid, three different fractions could be isolated from which the acidic pendant ratio (x) was determined (see method in §5). This determination led to different values of x, between 0.48 to 0.30 for the high to low molar mass fractions. These results clearly show that the crude copolymers have a heterogeneity in the degree of functionalization and that the high molar mass polymers are the most substituted. Incomplete reactions cannot be blamed for this because each of the polymer-analogous reactions we used had been checked to be quantitative. More probably, the heterogeneity problem comes from the starting poly(dimethylsiloxane-co-methylhydrogenosiloxane), the manufacturer ensuring the average ratio of methylhydrogenosiloxane units (x), not its degree of heterogeneity. It was not possible to reduce the dispersity in the ratio of the pendants, and therefore the fractionated SGLC copolymers were used and characterized as they were.

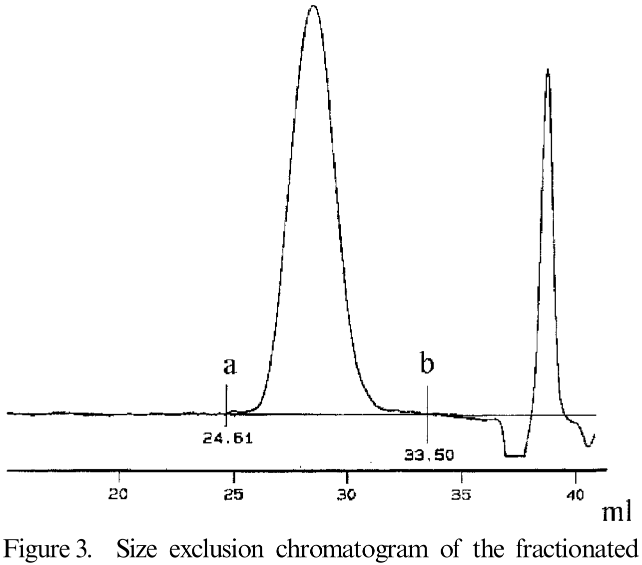

Figure 3. Size exclusion chromatogram of the fractionated copolyacid COPS 11-COOH. a and b are the limits for the determination of M_n and I_p.

3.2. *Mesomorphic properties*

The phase behaviour of the liquid crystalline copolysiloxanes is presented in table 2. The transition temperatures of their homopolysiloxane analogues are also given for comparison. The reported clearing temperatures and the SmA–SmC* transition temperatures correspond to the first appearance of the mesophase observed on cooling by optical microscopy. The glass transition temperature (T_g) and the transition temperatures to the highly ordered phase SmX were obtained by DSC.

The SGLC copolysiloxanes exhibit much clearer optical textures with larger monodomains than their homopolysiloxane counterparts [25]. The same mesomorphic sequence I–SmA–SmC*–SmX has been observed for both series of polysiloxanes. SmX corresponds to an unidentified high ordered phase. The effect of the fractionation of the copolyacid led to the copolysiloxane (*R*)-COPS 11-8 which presents the same phase sequence

Table 2. Transition temperatures for the sulphinate-based SGLC copolysiloxanes (*R*)-COPS 11-*n* and homopolysiloxanes (*R*)-PS 11-*n*. Polymers are unfractionated when not mentioned. ee = enantiomeric excess, SmX = unidentified high ordered phase.

			phase transition temperatures/°C								
Series of polymers	Name	%ee	g		SmX		SmC*		SmA		I
Copolysiloxanes	(*R*)-COPS 11-8	85	•	[a]	•	64	•	133	•	186	•
	(*R*)-COPS 11-8 (fractionated)	85	•	[a]	•	92	•	132	•	175	•
	(*R*)-COPS 11-10 (fractionated)	90	•	[a]	•	102	•	121	•	164	•
	(*R*)-COPS 11-12 (fractionated)	92	•	[a]	•	101	•	110	•	154	•
Homopolysiloxanes	(*R*)-PS 11-8	90	•	19	•	96	•	150	•	197	•
	(*R*)-PS 11-10	91	•	13	•	104	•	142	•	185	•
	(*R*)-PS 11-12	91	•	13	•	105	•	122	•	172	•

[a] Not found.

as the crude (unfractionated) copolymer COPS 11-8. However, the fractionated sample exhibits a lower clarification temperature (175 versus 186°C) and a much higher SmX–SmC* transition temperature (92 versus 64°C). In spite of our efforts to prepare well-defined copolysiloxanes, the fractionation of the copolyacid could not significantly reduce the temperature range of the biphasic region at the clarification temperature of the final SGLC copolymers. A biphasic gap over 30°C was still observed optically for all the series of SGLC copolysiloxanes. It has to be mentioned that the series of SGLC homopolysiloxanes does not show such wide biphasic regions during clarification. As explained in §3.1, the wide biphasic gap at the I–SmA transition in the copolysiloxanes most probably reflects the heterogeneity in the degree of functionalization *x* present in the starting poly(dimethylsiloxane-co-methylhydrogenosiloxane). This could be clearly observed by differential scanning calorimetry experiments, as seen for example, in the DSC trace of copolysiloxane (*R*)-COPS 11-10, presented in figure 4. This DSC trace has to be compared with the one corresponding to the homopolysiloxane (*R*)-PS 11-8 shown in figure 5. Thermal gravimetric analysis was also performed for one polymer of the series of homopolysiloxanes, (*R*)-PS 11-8. This thermogram, presented in figure 6, shows thermal stability over the entire mesophorphic temperature range of the polymer. The existence of a degradation process is observed after complete clarification of the polymer studied (200°C, under nitrogen). The mass loss calculated (about 15%) seems to reflect a cleavage of the alkyl chain connected to the sulphinate moiety.

As previously mentioned, the LC copolysiloxanes (*R*)-COPS 11-*n* exhibit the same phase sequence as the homopolysiloxanes (*R*)-PS 11-*n*. In table 2, the phase transition temperatures for both series of polymers are presented. The reported I–SmA and SmA–SmC* transition temperatures correspond to the upper limit of the biphasic regions. These transitions are clearly observed by optical microscopy and appear to be reproducible and associated with less than a 2°C thermal hysteresis. The SmC*–SmX phase transitions occur at

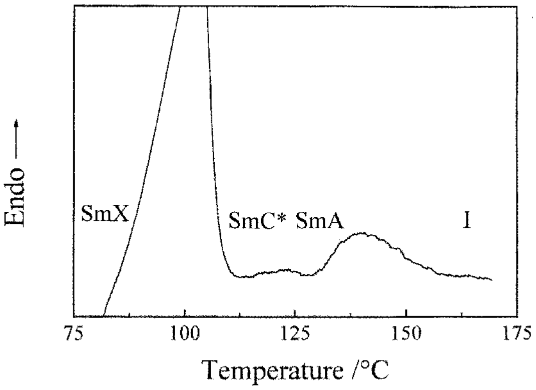

Figure 4. DSC trace for the copolysiloxane (*R*)-COPS 11-10, recorded on heating at 10°C min^{-1}.

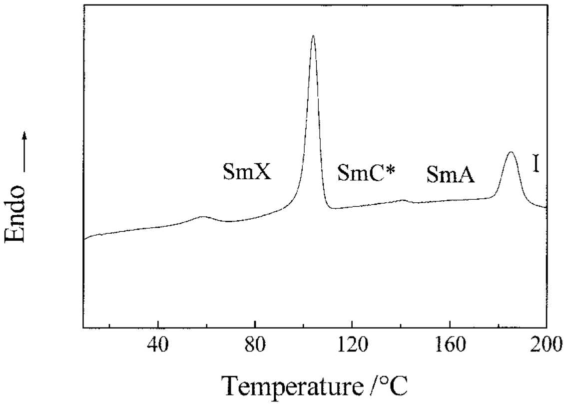

Figure 5. DSC trace for the homopolysiloxane (*R*)-PS 11-8, recorded on heating at 10°C min^{-1}.

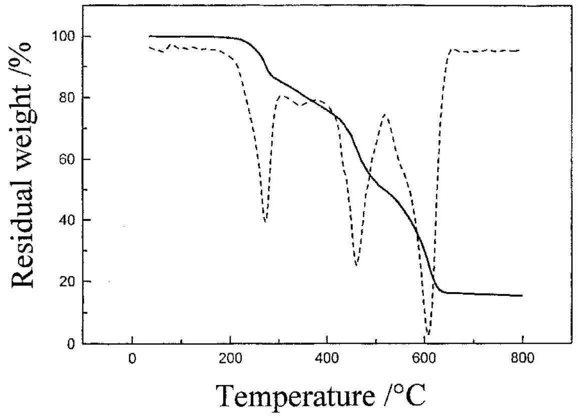

Figure 6. Thermogravimetric analysis of homopolysiloxane (*R*)-PS 11-8. (—): residual weight; (---): residual weight derivative.

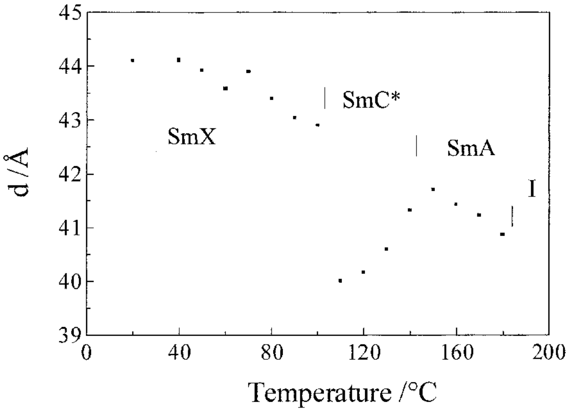

Figure 7. Temperature dependence of the layer spacing for the homopolymer (*R*)-PS 11-10.

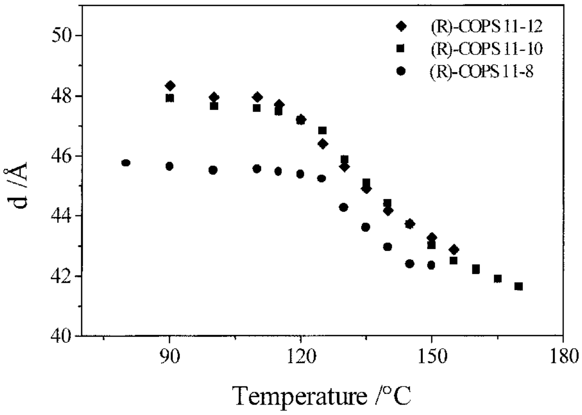

Figure 8. Temperature dependence of the layer spacing for the series of copolymers (*R*)-COPS 11-*n*.

nearly the same temperature (about 100°C) in both series of polymers. However, and according to the well-known 'dilution effect' [28, 29], the I–SmA and the SmA–SmC* transition temperatures appear at temperatures about 20°C lower in copolymers than in homopolymers. With respect to the terminal alkyl chain, lengthening the paraffinic chain produces the usual destabilization tendency of the mesomorphic properties in both series of polymers [30]. Due to this, there is a decrease in the I–SmA and SmA–SmC* phase transition temperatures of the polymers when going from the octyl to the dodecyl terminal chain.

X-ray diffraction experiments have been carried out for one homopolymer, (*R*)-PS 11-10, and for all copolymers of the series (*R*)-COPS 11-*n*. The X-ray patterns of the SmC* and SmA phases exhibit as usual first, one or two sharp Bragg reflections in the small angle region corresponding to the lamellar stacking, and second, a diffuse band in the wide angle region corresponding to the liquid-like arrangement of the pendant groups within the layers. Regarding the SmX phase, besides the reflections due to the lamellar ordering, the wide angle region of the X-ray pattern exhibits several Bragg peaks (rather diffuse) indicationg a more pronounced order within the layers. Figures 7 and 8 present the temperature dependence of the layer spacing *d* for the homopolymer and the copolymers, respectively. As a reference, the molecular length *l* of the mesogenic pendant with a terminal decyl chain (including a methylsiloxane unit) has been determined by molecular modelling to have a value of 43.5 Å in its minimized conformational energy state.

On decreasing the temperature of the homopolymer (*R*)-PS 11-10 (figure 7), a linear temperature dependence of the layer spacing *d* is observed in the SmA phase. Then, at the SmA–SmC* transition a strong and continuous decrease of *d* is observed, reflecting the usual increasing tilt angle of the mesogens in the SmC phase. At low temperatures, an increase of the layer spacing occurs in the SmX phase and the values tend to saturate at about 44 Å at room temperature. According to the calculated *l* and to the layer spacing variation *d*, these spacings are in agreement with a non-tilted arrangement of the mesogens in the low temperature phase of (*R*)-PS 11-10. This later phase could be attributed either to a crystalline phase or to a highly ordered smectic phase.

Regarding the copolymers, an unusual feature in the temperature dependence of the layer spacing is observed (figure 8): on decreasing the temperature from the isotropic state, an increase of *d* occurs in the SmA phase which then stabilizes and remains unchanged down to room temperature. This behaviour can be interpreted in terms of the heterogeneity in the ratio of the mesogenic pendants already discussed in §3.1 and above. Indeed, our copolysiloxanes (*R*)-COPS 11-*n* have to be considered as mixtures of copolymers with different pendant ratios. Smectic domains with large contents of highly substituted fractions will therefore exhibit higher transition temperatures than domains with large contents of lower substituted fractions. Indeed, X-ray diffraction carried out on partially substituted polymers [28, 31] showed that the layer spacing increases with decreasing substitution ratio (this behaviour indicates that the segregation of the unsubstituted units in the polymer backbone sublayer occurs without significant change in the close packing of the mesogenic pendants). In the present case, this would imply that the average layer spacing should increase over all smectic domains with decreasing average substitution ratio (and temperature) within the SmA phase, in a manner consistent with the experimental variation. Moreover, the absence of any significant *d* variation in the SmC* phase, in spite of the change in the tilt angle, strongly suggests that biphasic domains from the I–SmA and SmA–SmC* transitions overlap, both contributions compensating each other. Below this overlapping region and before the transition to the SmX or X phase, the invariance in the *d* spacing could be explained by the saturation of the tilt angle variation.

3.3. *Ferroelectric properties*

A complete characterization of the ferroelectric properties was carried out for the copolymers, which were found to be more thermally stable and easily alignable than their homopolymer counterparts. Measurements of the spontaneous polarization were performed on a calibrated standard bench by applying a triangular wave voltage across the surface-stabilized ferroelectric liquid crystal (SSFLC) cells filled with the copolymers. Due to the high transition temperatures and in order to avoid possible degradation of the materials, the SSFLC cells were not filled by the usual capillary effect. They were constructed by pressing and shearing a small amount of copolymer in the disordered mesophases, between ITO-covered substrates previously rubbed with a teflon rod in order to induce a planar alignment of the director in the rubbing direction [32]. In order to control the final thickness of the cells, 20 μm thick mylar film strips were placed between the substrates. The cells were digitally scanned in order to calculate their area. Due to the relatively high viscosity, these materials presented large switching times making it difficult to perform the spontaneous polarization measurements. A 10 Hz triangular wave voltage was used and the response signal averaged in order to reduce random noise. All data were taken on cooling the SSFLC cells from the SmA phase. The experimental variations are presented as a function of the difference in temperature ($T-T^*_{AC}$) with respect to the upper limit of the biphasic domain corresponding to the SmA–SmC* phase transition.

In figure 9 we present the spontaneous polarization values obtained by integrating the induced polarization current pulses, after eliminating the capacity and ionic components of the current. As can be seen, there is some data scattering due the experimentally limiting working conditions. However, it is clear that the spontaneous polarization for (*R*)-COPS 11-8 and for (*R*)-COPS 11-10 is higher than that for the (*R*)-COPS 11-12. In all cases it increases, with temperature decrease, up to saturation at values between 50 and 120 nC cm^{-2}. It is observed that the spontaneous polarizations obtained for (*R*)-COPS 11-8 and (*R*)-COPS 11-10 are equivalent to the values obtained for low molar mass sulphinate-based mesogens (for ee ~ 85%) [22, 23], but are much smaller than the values obtained for their organosiloxane analogues (saturation at values up to 250 nC cm^{-2} for ee ~ 90%) [33]. Moreover, the experimental variation in $\mathbf{P}_s$ could be consistent with an overlapping of I–SmA and SmA–SmC* biphasic domains. The nearly constant polarization observed for larger $T-T^*_{AC}$ values strongly suggests that the biphasic regions have been crossed and that the tilt angle has reached its saturation value.

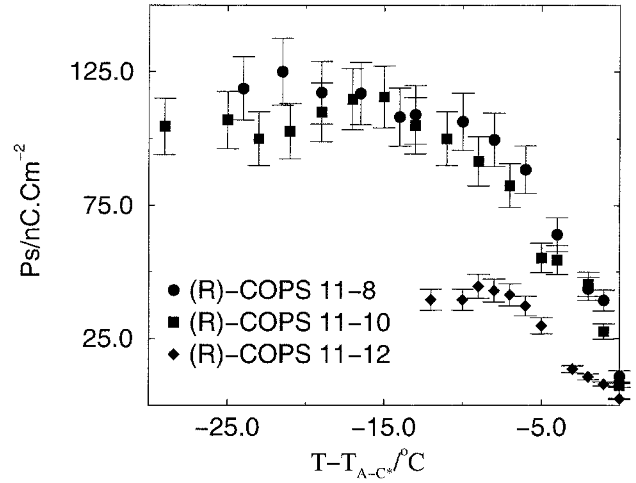

Figure 9. Spontaneous polarization versus reduced temperature for the copolymers (*R*)-COPS 11-*n*.

For the three copolymers, we present in figure 10 the switching time (τ) as a function of temperature, calculated from the induced polarization current pulses [34]. In all cases τ increases with decreasing temperature. The estimated values are in the range 1–4 ms. These values are of same order of magnitude as for other previously reported side group copolysiloxanes [28, 29, 35], and are higher by 2 to 3 orders of magnitude than those obtained for low molar mass siloxane materials [33, 35–39].

It is finally worth noticing that the spontaneous polarization decreases and the switching time increases with lengthening of the aliphatic chains according to the dilution of the mesogens and may be due to an increase of the viscosity.

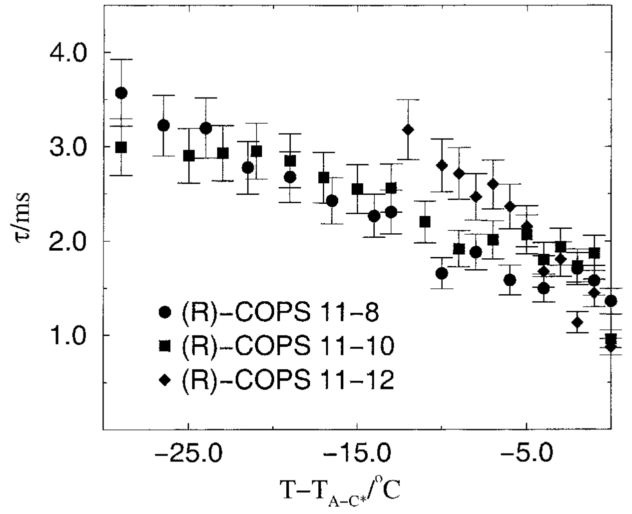

Figure 10. Response time versus reduced temperature for the copolymers (*R*)-COPS 11-*n*.

4. Summary

The present paper reports the synthesis and characterization of a series of ferroelectric sulphinate-based liquid crystalline homo- and co-polysiloxanes. In these materials, the chirality is introduced via an asymmetric sulphur atom. The polymers could be synthesized by using three efficient polymer-analogous reactions. All the polysiloxanes exhibit the ferroelectric SmC* mesophase. Its thermal stability depends on the type of polymer (homo- and co-polysiloxanes) and depends upon the length of the terminal alkyl chain on the mesogenic pendant. Unlike the homopolysiloxanes, the copolysiloxanes exhibit large biphasic regions at the transition temperatures, which appear to be due to a high heterogeneity in the mesogenic pendant ratio. This heterogeneity most probably originates from the commercial poly(dimethylsiloxane-co-methylhydrogenosiloxane) used as starting material for our syntheses. This intrinsic feature of the copolysiloxanes gives rise in particular to a singular temperature dependence of the layer spacing. Finally, characterization of the ferroelectric properties of the copolymers revealed high spontaneous polarization values.

5. Experimental

5.1. *Apparatus and techniques*

The values of the number-average molar mass (M_n) and the polydispersity index (I_p) were obtained by gel permeation chromatography (GPC). For the starting poly(dimethylsiloxane-co-methylhydrogenosiloxane), Ultrastyragel Waters columns (10^4, 10^3 and 500 Å, toluene, refractive index detection) were used, with well-defined poly(dimethylsiloxane) standards (tonometry). For the other polymers, PLgel mixed-D (weight separation domain: 200–400.000, tetrahydrofuran, UV detection) was used, with polystyrene standards. The average ratio of the functionalized siloxane units (x) on the polymers was calculated from careful investigation of the ^{1}H NMR spectra. For the copolyacide COPS 11-COOH, x was determined from titration of the COOH groups, by using tetrabutylammonium hydroxide (TBAH) with detection by potentiometry.

^{1}H NMR spectra (200 MHz) were recorded on a Bruker NR/200 AF spectrometer. Thermogravimetry was conducted on powdered samples using a Mettler TC10A instrument with a nitrogen atmosphere. The transition temperatures were measured by using both a polarized optical microscope equipped with a Mettler FP82 hot stage, and a differential scanning calorimeter Perkin-Elmer DSC-7 (heating and cooling runs of 10°C min^{-1}). X-ray diffraction experiments were carried out on powder samples in Lindemann capillaries with an Inel CPS 120 curved position-sensitive detector from an Inel X-ray generator, the sample temperature being controlled within ± 0.01°C.

5.2. *Synthesis*

5.2.1. *Hydrosilylation*

The starting poly(dimethylsiloxane-co-methylhydrogenosiloxane) was purchased from Petrarch Inc. (PS123, given for $M_n = 2000$–2100 and a 30–35% methylhydrosiloxane repeat unit content). The vinylic derivative 4-methoxybenzyl 4-(10-undecenyloxy)benzoate (8.89 g, 21.7 mmol) and the polysiloxane (3.12 g, 14.5 mmol Si–H) were added to 30 ml of anhydrous toluene. The reaction mixture was heated at 80°C under argon, and 575 µl of a solution of dicyclopentadienyl platinum (II) dichloride (2 mg ml^{-1} in dry dichloromethane, 200 ppm as referred to Si–H) was injected into the vessel. After a one day reaction time, 200 ppm more catalyst were added and the solution was heated at 100°C for two more days. The reaction mixture was cooled and filtered through a 0.45 µm pore size filter; then the polymers were isolated by five successive precipitations into methanol from a dichloromethane solution. After drying for 24 h at 60°C under vacuum, the polymer appears as a viscous oil, yield 65%. As checked by TLC and ^{1}H NMR, the polymer obtained was free from any residual vinylic derivatives. ^{1}H NMR, CDCl$_3$, δ (ppm): 7.99 (d, 2H, Ar–H); 7.38 (d, 2H, Ar–H); 6.89 (d, 2H, Ar–H); 6.86 (d, 2H, Ar–H); 5.26 (s, 2H, $-CH_2-Ar$); 3.97 (t, 2H, $-CH_2-O-$); 3.81 (s, 3H, $-O-CH_3$); 1.75 (m, 2H, $-C\underline{H_2}-CH_2-O-$); 1.50–1.15 (m, 16H, aliphatic protons); 0.51 (m, 2H, $-Si-CH_2-$), 0.08–0.04 (m, 13.6H, $-Si-CH_3$).

5.2.2. *Hydrogenolysis*

A suspension of 10% Pd/C (1.9 g) in 35 ml of dry tetrahydrofuran was charged with the polymers previously prepared (5.60 g, 26.3 mmol of benzyl groups). Slight hydrogen bubbling was allowed into the stirred mixture for 2 days at 25°C. The reaction mixture was filtered through celite, then through a 0.45 μm pore size filter. The filtrate was concentrated and precipitated twice into pentane from a tetrahydrofuran solution to give a white precipitate which was dried *in vacuo*, yield 85%. ^{1}H NMR, tetrahydrofuran-d$_8$, δ (ppm): 8.07 (d, 2H, Ar–H); 7.05 (d, 2H, Ar–H); 4.14 (t, 2H, $-CH_2-O-$); 2.1–1.15 (m, 18H, aliphatic protons); 0.72 (m, 2H, $-Si-CH_2-$); 0.08–0.04 (m, 14.8H, $Si-CH_3$). The absence of any trace of a peak at 5.2 ppm (corresponding to the benzylic protons) revealed that the deprotection step was complete. The evaluation of the ratio of benzoic acid groups (TBAH reagent, detection by a potentiometric method) gave 9.37% (calculated for $DP = 29.5$ and $x = 0.38$: 9.05%).

5.2.3. *Polyesterification*

The general procedure for the preparation of the final SGLC copolysiloxanes is as follow: a flask fitted with a calcium chloride drying tube was charged with the 'acidic' copolysiloxane (270 mg, 0.54 mmol of carboxylic acid functions), the sulphinate derivative (1.1 mmol) and dimethylaminopyridinium *p*-toluenesulphonate (DPTS) (48 mg, 0.16 mmol). The mixture was first solubilized with 1 ml of dry tetrahydrofuran, and 2 ml of dry dichloromethane were added to the solution. The reaction mixture was cooled to 0°C with an ice-water bath, and dicyclohexylcarbodiimide (DCC) (225 mg, 1.1 mmol) in 3 ml of dichloromethane was then introduced. After 1 h, the ice-water bath was removed and the mixture was kept stirring for 3 days at room temperature. The precipitate of dicyclohexylurea was filtered off and the filtrate concentrated. The residue was solubilized in a minimum of toluene and the solution filtered through a 0.45 μm pore filter. Two successive precipitations in methanol from tetrahydrofuran solution were enough to obtain the polymers free from any residual low molecular mass materials, as checked by thin layer chromatography. The polymers were finally dried for 2 days at 40°C under vacuum, and appeared as white solids, yield 70–85%.

Typical ^{1}H NMR spectra obtained for (*R*)-COPS 11-8. $CDCl_3$, δ (ppm): 8.12 (d, 2H, Ar–H); 7.68 (s, 4H, Ar–H); 7.58 (d, 2H, Ar–H); 7.22 (d, 2H, Ar–H); 6.96 (d, 2H, Ar–H); 4.05 (m, 2H, $-CH_2-O-$ and 1H, $SOO-CH_2-$); 3.61 (m, 1H, $SOO-CH_2-$); 1.90–1.10 (m, 30H, aliphatic protons); 0.85 (t, 3H, $-O-CH_3$); 0.51 (m, 2H, $-Si-CH_2-$); 0.12–0.04 (m, 14.3H, $-Si-CH_3$).

For all polymers, the quantitative determination of the residual benzoic acid moieties (TBAH reagent, detection by a potentiometric method) was found to be 0.00%. The polyesterification was then concluded to be quantitative.

Elemental analysis: calc. (found) for polymer (*R*)-COPS 11-8, for $DP = 29.5$ and $x = 0.38$: Si 9.45 (9.37), C 64.15 (64.16), H 7.87 (7.83), S 3.81 (3.85)%.

Elemental analysis: calc. (found) for polymer (*R*)-COPS 11-10, for $DP = 29.5$ and $x = 0.38$: Si 9.22 (9.23), C 64.84 (64.37), H 8.08 (8.16), S 3.68 (3.57)%.

Elemental analysis: calc. (found) for polymer (*R*)-COPS 11-12, for $DP = 29.5$ and $x = 0.38$: Si 8.86 (8.80), C 65.50 (65.35), H 8.27 (8.28), S 3.57 (3.48)%.

The authors are very thankful to Dr Y. Galerne for fruitful discussions and to L. Oswald for her technical assistance. P. S. is grateful to the projects ERBCHR XCT 930353, FCT PBIC/C/CTM/1936/95 and PRAXIS XXI 3/3.1/MMA/1769/95 for financial support.

References

[1] Coates, D., 1987, in *Thermotropic Liquid Crystals*, edited by G. W. Gray (John Wiley & Sons), p. 99.

[2] Dübal, H.-R., Escher, C., and Ohlendorf, D., 1988, *Ferroelectrics*, **84,** 143.

[3] Bahr, C., Heppke, G., and Sabaschus, B., 1988, *Ferroelectrics*, **84,** 103.

[4] Cherkaoui, M. Z., Nicoud, J. F., Galerne, Y., and Guillon, D., *Liq. Cryst.*, in press.

[5] (*a*) Goodby, J. W., 1991, in *Ferroelectric Liquid Crystals* (Gordon & Breach Science Publishers), p. 158; (*b*) Goodby, J. W., 1998, invited lecture at the 17th International Liquid Crystal Conference, 19–24 July, 1998, Strasbourg.

[6] Kelly, S. M., 1998, in *Handbook of Liquid Crystals*, Vol. 2B, edited by D. Demus, J. Goodby, G. W. Gray, H. W. Spiess, and V. Vill (Wiley-VCH). Chap. VI.

[7] See, for example, (*a*) Sierra, T., Serrano, J. L., Ros, M. B., Ezcurra, A., and Zubia, J., 1992, *J. Am. chem. Soc.*, **114,** 7645; (*b*) Wang, Q., Fan, S. Y., Wong, H. N. C., Li, Z., Fung, M., Twieg, R. J., and Nguyen, H. T., 1993, *Tetrahedron Lett.*, **49,** 619; (*c*) Colquhoun, H. M., Dudman, C. C., O'Mahoney, C. A., Robinson, G. C., and Williams, D. J., 1990, *Adv. Mater.*, **2,** 139; (*d*) Suzuki, Y., Nonaka, O., Koide, Y., Okabe, N., Hagiwara, T., Kawamura, I., Yamamoto, N., Yamada, Y., and Kitazume, T., 1993, *Mol. Cryst. liq. Cryst.*, **147,** 109.

[8] Solladié, G., and Zimmermann, R. G., 1985, *Angew. Chem. int. Ed. Engl.*, **24,** 64.

[9] Yamamura, K., Okada, Y., Ono, S., Watanabe, M., and Tabushi, I., 1988, *J. chem. Soc., chem. Commun.*, 443.

[10] Zhang, Y., and Schuster, G. B., 1994, *J. org. Chem.*, **59,** 1855.

[11] Bhatt, J. C., Keast, S. S., Neubert, M. E., and Petschek, R. G., 1995, *Liq. Cryst.*, **18,** 367.

[12] Solladié, G., Hugelé, P., Bartsch, R., and Skoulios, A., 1996, *Angew. Chem. int. Ed. Engl.*, **35,** 1533.

[13] Lunkwitz, R., Tschierske, C., Langhoff, A., Giesselmann, F., and Zugenmaier, P., 1997, *J. mater. Chem.*, **7,** 1713.

[14] (*a*) Poths, H., Zentel, R., Vallerien, S. U., and Kremer, F., 1991, *Mol. Cryst. liq. Cryst.*, **203,** 101; (*b*) Poths, H., Zentel, R., Kremer, F., and Siemensmeyer, K., 1992, *Adv. Mater.*, **4,** 351.

[15] (*a*) Ziminski, L., and Malthète, J., 1990, *J. chem. Soc., chem. Commun.*, 1495; (*b*) Jacq, P., and Malthète, J., 1996, *Liq. Cryst.*, **21,** 291.

[16] Potentially optically active ferrocenyl-based liquid crystals: Descheneaux, R., and Santiago, J., 1994, *Tetrahedron Lett.*, **35,** 2169.

[17] Nishide, K., Nakayama, A., Kusumoto, T., Hiyama, T., Takehara, S., Shoji, T., Osawa, M., Kuriyama, T., Nakamura, K., and Fujisawa, T., 1990, *Chem. Lett.*, 623.

[18] Soldera, A., Nicoud, J. F., Galerne, Y., Skoulios, A., and Guillon, D., 1992, *Liq. Cryst.*, **12,** 347.

[19] Ribeiro, A. C., Dreyer, A., Oswald, L., Nicoud, J. F., Soldera, A., Guillon, D., and Galerne, Y., 1994, *J. Phys. II Fr.*, **4,** 407.

[20] Soldera, A., Nicoud, J. F., Skoulios, A., Galerne, Y., and Guillon, D., 1994, *Chem. Mater.*, **6,** 625.

[21] Cherkaoui, M. Z., Nicoud, J. F., and Guillon, D., 1994, *Chem Mater.*, **6,** 2026.

[22] Cherkaoui, M. Z., Nicoud, J. F., Galerne, Y., and Guillon, D., 1995, *J. Phys. II Fr.*, **5,** 1263.

[23] Cherkaoui, M. Z., Nicoud, J. F., Galerne, Y., and Guillon, D., 1997, *J. chem. Phys.*, **106,** 7816.

[24] (*a*) Angeloni, A. S., Laus, M., Caretti, D., Chiellini, E., and Galli, G., 1991, *Chirality*, **3,** 307; (*b*) Chiellini, E., Galli, G., Angeloni, A. S., Laus, M., Melone, S., and Francescangeli, O., 1993, *Mol. Cryst. liq. Cryst.*, **266,** 189; (*c*) Laus, M., Angeloni, A., Galli, G., Chiellini, E., Francescangeli, O, and Yang, B., 1995, *Polymer*, **36,** 1261.

[25] Méry, S., Nicoud, J. F., and Guillon, D., 1995, *Macromolecules*, **28,** 5440.

[26] (*a*) Descheneaux, R., Kosztics, I., Sholten, U., Guillon, D., and Ibn-Elhaj, M., 1994, *J. Mater. Chem.*, **4,** 1351; (*b*) Descheneaux, R., Turpin, F., and Guillon, D., 1997, *Macromolecules*, **30,** 3759.

[27] Nicoud, J. F., and Cherkaoui, M. Z., 1995, *Tetrahedron: Asymmetry*, **6,** 1941.

[28] Dumon, M., Nguyen, H. T., Mauzac, M., Destrade, C., Achard, M. F., and Gasparoux, H., 1990, *Macromolecules*, **23,** 357.

[29] Poths, H., and Zentel, R., 1994, *Liq. Cryst.*, **16,** 749.

[30] Percec, V., and Pugh, C., 1989, in *Side Chain Liquid Crystal Polymers*, edited by C. B. McArdle (Glasgow and London: Blackie), p. 30.

[31] Descheneaux, R., Jauslin, I., Scholten, U., Turpin, F., Guillon, D., and Heinrich, B., 1998, *Macromolecules*, **31,** 5647.

[32] Wittmann, J. C., and Smith, P. 1991, *Nature*, **352,** 414.

[33] Sebastião, P., Méry, S., Sieffert, M., Nicoud, J. F., Galerne, Y., and Guillon, D. 1998, *Ferroelectrics*, **212,** 133.

[34] Skarp, K., and Handschy, M. A., 1988, *Mol. Cryst. liq. Cryst.*, **165,** 439

[35] Poths, H., Winscherhoff, E., Zentel, R., Schönfeld, A., Henn, G., and Kremer, F., 1995, *Liq. Cryst.*, **18,** 811.

[36] Coles, H. J., Owen, H., Newton, J., and Hodge, P., 1993, *Liq. Cryst.*, **15,** 739.

[37] Redmond, M., Coles, H., Wischerhoff, E., and Zentel, R., 1993, *Ferroelectrics*, **148,** 323.

[38] Naciri, J., Pfeiffer, S., and Shashidhar, R., 1991, *Liq. Cryst.*, **10,** 585.

[39] Helgee, B., Hjertberg, T., Skarp, K., Andersson, G., and Gouda, F., 1995, *Liq. Cryst.*, **18,** 749.